International Journal of Chemical and Biochemical Sciences
(ISSN 2226-9614)

Journal Home page: www.iscientific.org/Journal.html

Role of human dental pulp stem cells and HA /PLGA porous scaffold in regeneration of mandibular bone defect in rabbit

Khalaf Afaf Ali[1], Shamaa Ali [2] Sabry Dina Abd El Fattah [3], Saher S Mohammed [4]*

[1]*Faculty of Dentistry, Minia University, Egypt*

[2]*Faculty of Dentistry, kafr elsheik University, kafr elsheik, Egypt*

[3]*Faculty of Medicine, Cairo University, Egypt*

[4]*Faculty of Dentistry, Minia University Minia, Egypt*

Abstract

Recently, a greater interest in tissue engineering for the treatment of large bone defects has been reported. Teeth are the most natural, noninvasive source of stem cells. Human dental pulp-derived mesenchymal stem cells (HDP-MSCs) offer a promising source of progenitor cells for regenerative medicine and bone tissue engineering. Scaffolds PLGA and HA stimulate cell proliferation and differentiation and play major roles in providing growth and nutrition factors in the repair of bone defects. A total of 18 mandibular defects were made, and three groups (each n = 6) were created. The first group: the transplanted DPSCs implanted in the critical-sized bone defect after receiving (HA/PLGA) scaffold. The second group received only (HA/PLGA) scaffold. The third group, which served as the control, had a critical-sized defect left empty. After characterization, Von Kossa [VK] and Alizarin red staining were employed to identify differentiated osteoblasts at the 14th and 21st days, and histological analyses, as well as polymerase chain reactions (PCR), were also used. Specimens were collected and evaluated by microradiology and histological analysis. It showed that DPSCs had high proliferation potential and typical fibroblastic shape. Additionally, osteogenic differentiation of DPSCs was validated by morphological alterations, histological examination, and the expression of lineage-specific genes confirmed osteogenic differentiation of DPSCs. High proliferation potential and the capacity to differentiate into osteoblasts are two characteristics of DPSCs taken from impacted third molars.

Keywords: dental pulp stem cells; synthetic scaffold; bone regeneration; tissue engineering.

Full length article **Corresponding Author*, e-mail: *afaf khalaf 434@ gmail.com; afaf khalaf 434@gmail.com*

1. Introduction

Bone defects represent a medical and socioeconomic challenge. Different types of biomaterials are applied for reconstructive indications and receive rising interest. Autologous bone grafts are still considered the gold standard for the reconstruction of extended bone defects. However, the morbidity of the procedure remains a drawback that has driven the development of new technical means to improve the therapeutic effect [1]. Although bone is a highly vascularized tissue and has the ability to regenerate, beyond a critical point, clinical intervention measures are required. It is hoped that bone tissue engineering [BTE] will be the future treatment of choice, as it will likely eliminate many of the pitfalls of current treatments [2]. In this study, we discuss the status and key issues for BTE components (i.e., biomaterials, cells, signaling molecules, and vascularization). Tissue engineering [TE] is “an interdisciplinary field of research that applies the principles of engineering and the life sciences towards the development of biological substitutes that restore, maintain, or improve tissue function." In contrast to the classic biomaterials approach, it is based on an understanding of tissue formation and regeneration and aims to induce new functional tissues rather than just implant new spare parts [3]. The manufacture of superior tissue-engineering constructs depends on three basic elements: appropriate scaffolds to support tissue-cell regeneration, cytokines, and appropriate seed cells [4]. For a successful result, all of these single-cell components have to be combined in a well-coordinated spatial and time-dependent fashion. Furthermore, all of them should possess a number of properties and characteristics that make them suitable for this purpose [5]. To treat large-scale bone defects, the development of three-dimensional (3D) porous scaffolds, which act as a template for cell attachment and stimulate functional bone tissue formation in vivo through

tailored biophysical cues to direct the organization and behavior of cells [6]. A critical first step in creating a tissue-engineered product is choosing the best material for the scaffold, where the material's characteristics will largely dictate the scaffold's characteristics [7]. The next step after the development of an adequate porous structure is the choice of a reliable source of cells that allows their isolation and expansion into high numbers. Furthermore, in certain bone-related diseases, osteoblast cells may not be appropriate for transplantation because their protein expression profile is below the expected values [8]. Mesenchymal stem cells (MSCs) have been demonstrated as an attractive cell source for tissue engineering applications because of their ability to be easily isolated and expanded from adult bone marrow aspirates and their versatility for pluripotent differentiation into mesenchymal tissues [9]. The adult human dental pulp stem cells (hDPSCs) is the source of a unique population of stem cells that we have specifically chosen for this study. These cells can self-expand and differentiate into mesenchymal-derived cells such as adipocytes, myotubes, and osteoblasts, the latter of which can create 3D mineralized woven bone tissue in vitro. Additionally, we've shown that this tissue undergoes rapid lamellar bone remodeling in immunocompromised rats following in vivo transplantation [10].

2. Material and methods

2.1 Animals

A total of 18 New Zealand white rabbits, aged 3 months and with a weight range of 1.5–2 kg, were used in the present study. All animals were treated humanely under the ethics approval committee of Minia University. Rabbits were obtained and housed in cages in a cool room temperature out of direct sunlight and were protected from draughts, loud noises, and direct access to radiators in the animal house at the Faculty of Veterinary Medicine, Sohag University. Rabbits were fed a commercial pelleted rabbit diet.

A total of 18 mandibular defects were made and three experimental groups were formed: [n=6]

Group 1: The bone defect was filled with hydroxyapatite matrix and polylactic -polyglycolic acid (HA/PLGA) scaffold implanted with human dental pulp stem cells (DPSCs) for.

Group 2: The bone defect was filled with HA/PLGA scaffold only.

Group 3: The bone defect was left empty and served as a control group

All groups treated for 3 months.

2.2 Ethical consideration

All participants were informed about the practical steps of this study and signed consent. All experiments were reviewed and approved according to the guidelines for the responsible use of animals in research as a part of the scientific research ethics recommendation of the ethical Minia University (Approval 22/2/2021: [No. 486].

2.3 Surgical procedure

Every rabbit was fasted for 12 hours prior to surgery. Throughout the surgical procedure, general anesthesia was maintained via intramuscular injections of xylazine (5 mg/kg body weight) and ketamine hydrochloride (35 mg/kg body weight) [11]. A lancet was used to make an external incision in the mandibular base that was about 2 cm long, allowing for layer dissection. The subperiosteal flap was then extended to the muscle layers until it reached the bone. Using a hard drill #702 with a low-speed hand piece and continuous irrigation of sterile saline solution 0.9%, a circular critical-size defect measuring approximately 10 mm in diameter and 3 mm in height was created in all animal models. Utilizing a keen excavator, the bone tissue was extracted. Ultimately, the flaps were carefully repositioned and sutured (Fig. 1) following surgery [12].

2.4Methods

2.4.1 DPSCs Isolation and culture

The procedures that are mainly used by researchers in order to detect, isolate, proliferate, and differentiate DPSCs include the following. The teeth of healthy adults were used to extract human dental pulp. Every participant had their oral and systemic infections and illnesses examined before extraction. Only healthy individuals were chosen for the study. Every participant, who is typically a patient undergoing third molar extraction, adheres to a pretreatment plan involving professional dental hygiene. The dental crown was covered with 0.3% chlorexidin gel for two minutes prior to extraction in order to lower the microbial flora. A cylindrical turbine bur was used to make an incision at the cemento-enamel junction. In less than two hours, the pulp was carefully extracted using cow horn forceps and a small excavator while under sterilized conditions. It was then submerged in culture medium tubes and moved to the laboratory. The pulp was taken out and then submerged in a digestive solution (3 mg/mL type I). After filtration, cells were cultured in a culture medium usually Dulbecco's modified Eagle's medium [DMEM] supplemented with 10% Fetal bovine serum { FBS}, 2 mM L-glutamine, 100 U/mL penicillin, 100 µg/mL streptomycin, and placed in 75-cm3 2 flasks with filtered valves. Flasks were incubated at 37°C and 5% CO 2 and the medium changed twice a week. Just before cells become confluent, they could be subdivided into new flasks. The number of passages reached 3rd passage. Stem cells were reached at least 3,000,000 per flask. This number was achieved around day 21, when they were still undifferentiated. Dental pulp stem cell (DPSCs) will be characterized by flow cytometry at the third passage through the evaluation of the expression of the markers that define its phenotype as CD73, CD105, CD90, CD34, and CD45.

2.4.2 Assessment of Osteogenic Differentiation by Von Kossa and Alizarin red staining

For in vitro osteogenic differentiation, passage two DPSCs at a concentration of 5×104 cells were plated in 6-well tissue culture plates with complete expansion culture media. When DPSCs cultures became 80%-90% confluent, the primary culture medium was replaced by osteogenic induction medium (Osteo life LM-0023, LOT NO 05007) supplemented with 1% penicillin/streptomycin solution (Capricorn cat# PS-B, Cat no CP13-1019). Osteogenic differentiation medium was replaced with fresh media after every 3-5 days and experiments were terminated after 21 day [13]. The assessment of DPSCs differentiation into osteoblasts was determined by “Von Kossa” staining. Briefly, after 14 and 21 days of induction, the osteogenic

differentiation medium was discarded, and cells were fixed with 10% formalin for 15 minutes. Cells were stained using a commercially available Von Kossa staining kit (MASTER TEC STAIN KITS lot No. AAEWD005). Stained cultures were observed by bright field microscopy and images were captured [14]. In addition to Von Kossa Staining, the osteogenic induced cultures were also stained with alizarin red S (Cat no 22889). Differentiated DPSCs were fixed with 10% formalin for 15 minutes and were stained with 2% Alizarin Red S for 15-30 minutes. Cultures were then thoroughly washed with deionized water and viewed under light microscope [15].

2.4.3 HA/PLGA scaffolds Preparation

HA and PLGA (50/50) solutions were mixed (3:1 w/w ratio) in 0.2% chloroform at 25 °C for 24 h. Once mix and dissolve HA/PLGA solution was found to be spread on cylindrical replica mold during 2 h at -20 °C and then lyophilized. HA/PLGA scaffolds was cut into small cylinders (~ 9 mm in diameter and ~2 mm in height) which fit the area of the 24 wells. DPSCs (5 × 105, between passages 3 to 6) were seeded into the HA/PLGA scaffold and maintained in DMEM culture medium at 37 °C prior implementation in the critical sized bone defect of the animal model [16]. DPSCs when seeded into the HA/PLGA scaffold can be stored at 4°C for 24 h prior implementation in the critical sized bone defect of the animal model without any significant reduction of cell viability.

2.4.4 Polymerase chain reaction (PCR)

To evaluate the expression of lineage specific genes, polymerase chain reaction was performed. Briefly, RNA was isolated after day 14 and 21 of osteogenic induction by TRIZOL (Invitrogen) and cDNA was synthesized using reverse transcriptase (Wizscript cDNA synthesis kit) [17]. For PCR, WizPure™ PCR 2X Master Mix was used. Sequences for the primer pairs and their product lengths (bp) are given in Table 1:- Euthanasia was performed by anesthetic overdose (ketamine and xylazine) at the 3 months postoperative day. Immediately thereafter, the region of the critical-size bone defect area was removed and sent to the processing slides needed for further analysis.

2.4.5 Micro-computer tomography examination of samples

After sacrifice, the excised bone samples were transferred with a damp cloth to the center of [the Ora-scan. Sohag] for m-CT analysis. The samples were examined with a micro-computer tomography (m-CT) system (Fan beam Micro-CT). The micro focus of the X-ray source of the m-CT system had a spot size of 7 mm and a maximum voltage of 36 kV. The specimens were placed in a sample holder filled with water. They were oriented in such a way that the long axis of the block was parallel to the axis of the sample holder. A high-resolution protocol (slice thickness of 120 mm, feed of 60 mm, and pixel size of 60 mm) was applied. Depending on the length of the specimens, up to 180 slices were scanned perpendicular to the block. In addition, the ranges and means of the gray levels characteristic of the scaffold and newly formed bone were determined allowing reliable distinction between the two tissue types. Finally, -CT slices were compared with the corresponding histological slides to verify the reliability of the discrimination criteria [18].

2.5 Histopathological analysis

-After the micro-CT measurements, tissue samples were prepared for histological analysis. The samples were decalcified in Plank-Rychlo's solution (MUTO Pure Chemicals Co., Tokyo, Japan) for 5 days, dehydrated in graded ethanol baths, and then embedded in paraffin. The embedded samples were cut into 4-µm-thick sections using a microtome and stained with hematoxylin-eosin (HE; Sigma, St. Louis, MO) following standard protocols [19]. Stained slide images were acquired using a standard light microscope (Leica DM500, Leica Microsystems, Wetzlar, Germany) equipped with a SPOT digital camera (Diagnostic Instruments, Inc., Sterling Heights, MI, USA). In performing the histomorphometric analysis, four sites were randomly selected for each slide and the new bone formation area of each region was calculated using Image-Pro plus 6.0 software (Media Cybernetics, Silver Spring, MI, USA).

2.5.1 Immunohistochemistry analysis

Histological specimens (4-µm thick) were collected on silanized slides for better adhesion of the tissue sections studied and then kept in an oven for 24 hours at 37°C. After deparaffinization and hydration, histological sections were marked with a hydrophobic pen and then washed in a Tween enriched buffer solution twice for 3 minutes. Afterwards, the sections were immersed in a hydrogen peroxide for 10 minutes and then washed in phosphate buffer solution (PBS) twice in 3 minutes and finally immersed in inactivate endogenous peroxidase for 30 minutes. The samples were incubated with anti-Col-I (Santa Cruz Biotechnology, Dallas, TX, United States) polyclonal primary antibody at the concentration of 1:100, for 2 hours and afterwards were washed twice in PBS. They were then submitted to a secondary antibody (anti-rabbit IgG) (Vector Laboratories, Burlingame, CA, United States) at the concentration of 1:200 in PBS for 30 min. After this process, the samples were washed in PBS three times before application of the avidin-biotin complex conjugated with peroxidase (Vector Laboratories, Burlingame, CA, United States) for 45 minutes. Visualization of the bound complexes was performed with application of 0.05% 3'3 diaminobenzidine solution, and contrast was given by Harris hematoxylin (Vector Laboratories, Burlingame, CA, United States). The immunomarking of Collagen-I (Col-I) were qualitatively and semi-quantitatively evaluated. The qualitative analysis indicated the presence of a brownish immunostaining, and the semi-quantitative analysis was carried out by capturing three consecutive fields, using a light microscope (Leica Microsystems, Wetzlar, Germany). All analysis was performed by an experienced pathologist in a blind study [20].

2.5.2 Data analysis

The above data are presented as means ± standard deviations. Data analysis was performed using the SPSS 15.0 software (SPSS Inc., Chicago, IL, USA). The differences were considered significant when P values were <0.05 and highly significant when $P<0.01$ and $P<0.001$.

3. Results

3.1 Figure 2 [A-B]

Macroscopic and radiographic images of the implantation sites at 3 months: After the study period, the healing of the rabbit mandibular defect was observed macroscopically and assessed using a micro-computer tomography in both the treated and control groups.

3.2 Isolation and Characterization of human dental pulp-derived mesenchymal stem cells of[DPSCs]

Following 4–7 days in culture, the cells began to proliferate from the tiny tissue segments and adhere to the plastic surface. **Figure 3** illustrates how adherent cells formed a monolayer within three weeks of culture, reaching 70–80% confluency after about two weeks. MSCs were distinguished by their fibroblastic morphology and plastic adherent characteristics. By using FACS to characterize them, DPSCs were found to be negative for CD34 and CD45 and positive for CD90 and CD105.

3.3 Osteogenic differentiation potential of dental pulp derived mesenchymal stem cells DPSCs

In osteogenic induction medium, after14 and 21 days of induction, newly differentiated osteoblasts grew in multiple layers and stained positive for “Von Kossa” as well as “Alizarin red”, confirming the differentiation of DPSCs into osteoblasts. Alizarin red staining assay was performed for detection of the calcium deposits (mineral deposits) chelate with alizarin forming an alizarin red calcium complex detected as orange-red staining spots as shown in **fig 4.**

3.4 Real-Time Reverse Transcription Polymerase Chain Reaction (RT-PCR) Measures the mRNA Expression

The in vitro osteogenesis of differentiated DPSCs groups were determined by the mRNA expression of RUNX2, ON and COL1. The expression levels of several genes in groups of differentiated DPSCs were used as quantitative standards. When cells were seeded on PLGA/HA scaffolds, the osteoblast-specific transcription factor RUNX2 displayed high expression at days 15 and 30, which was significantly greater than in other treated and control groups [value was around 3.728516 ($p < 0.05$)]. Osteonectin [ON], another mineralization marker, was consistently expressed in all experimentally treated groups. In addition, the PLGA/HA/DPSCs group displayed a greater expression level (about 3.372864) than the other groups. Lastly, the differentiated DPSCs groups consistently had higher collagen1 expression than the other groups. [Approximately 3.56174 ($p < 0.05$)].

3.5 Histological analysis of bone regeneration

Histological evidence further supported the radiographic findings, indicating that the specimens of control group, the bone defect is filled mainly with connective tissue. In other words, no bony tissue is observed and only fibrous scar tissue formation is evident after 3months. PLGA/HA scaffold only group exhibited a large amount of blood clot in the central portion of the defect, and the presence of small foci of connective tissue in which it was possible to observe increased formation of immature trabecular bone at the margins of defects. Furthermore, PLGA/HA / +DPSC groups showed nearly complete osseous closure of the defect, where the newly formed bone had typical organized and mature bone morphology with Haversian systems and noticeable marrow spaces similar to native bone Moreover, osteocytes are seen in the newly-formed thickened bone. In addition, considerable numbers of osteoplastic cells can be seen on the surface of the newly-formed bone as shown in fig 5 [A-B-C]. Immunohistochemistry was performed to determine Collagen type I expression levels. Immunohistochemistry exhibited strong expression in areas of new bone formation within the defect region from samples treated with the PLGA/HA/HDPS whereas PLGA/HA staining were visible but much weaker. Moreover, No obvious positive staining was observed in the control group as shown in fig 5[D-E-F].

3.6 Morphometric assessment

Area Percentage of new bone formation and bone marrow in the critical sized of mandibular defects in the four experimental groups: -The mean and standard deviation values were calculated for each group in each test. Data were explored for normality using Kolmogorov-Smirnov and Shapiro-Wilk tests, data showed parametric (normal) distribution. One-way ANOVA followed by Tukey post-hoc test was used to compare between more than two groups in non-related samples. The significance level was set at $P \leq 0.05$. Statistical analysis was performed with IBM® SPSS® Statistics Version 20 for Windows. In the histomorphometric analysis, histological findings were confirmed, in which the treated groups presented a more advanced healing process, demonstrating greater new bone formation when compared to the control. Group [I] PLGA/HA/HDPMSCs presented 92.09%, group [II] PLGA/HA 65.16% and control group b39.28 % respectively. A statistically significant difference was found between (Group 1) and each of (Group II) and (Group III) where ($p<0.001$) and ($p<0.001$). Immunohistochemistry Collagen I results:- Immunohistochemistry Collagen I represents the semi-quantitative analysis of the Col-I performed through score. The results showed significant statistical differences between the amounts of collagen fibers present in each evaluated experimental group. Control group presented the highest amount of fibers in the experimental period (3 months) when compared to group PLGA/HA/HDPMSCs and group PLGA/HA where ($p<0.001$).

4. Discussion

The function of bone tissue engineering in regenerative medicine has been the focus of intense research over the last two decades. Technological advancements have enhanced bone repair surgery procedures and orthopedic implants [21]. However, advancements in surgical procedures for bone reconstruction have been hampered by a lack of autologous materials and donor site morbidity [22]. The use of osteoprogenitor cells and scaffolds that can be inserted in vivo at the location of the fractured bone has been recognized as a fascinating prospect for the repair of critical-sized bone defects, with MSCs currently considered to be the most suitable candidates for bone tissue engineering uses [23]. Dang et al., on the opposite hand, found that using stem cells on scaffolds significantly improved and accelerated bone healing [24]. A combination of mesenchymal stem cells and biosynthetic matrix (MSCs) was used. In the present study, homogenous hDPSCs with

defined characteristics of MSCs were transplanted with an HA/PLGA scaffold in the surgical field. We studied the effect of HA, PLGA, and HDPSCs on bone regeneration and observed promising results in the accelerated bone regeneration of large defects in the critical size of mandibular defects in rabbits in about 3 months. Because of its desired mechanical characteristics, biodegradability, and biocompatibility, PLGA is an FDA-approved synthetic polymer that has been widely employed for in vitro and in vivo bone regeneration investigations [25, 26]. Even though pure PLGA is biocompatible, its clinical usage for bone regeneration is limited by weak osteoconductivity and inadequate mechanical characteristics. As a result, PLGA is frequently combined with ceramics [HA] to make it more biomimetic and capable of enhancing the growth of bones for tissues engineering and regenerative medical applications [27]. Following primary culture, a subpopulation of cells (DPSCs) with spindle form, fibroblastic shape, and plastic adherent growth were found. MSC characterization standards are established by the International Society for Cellular Therapy (ISCT). These criteria revealed that the cells in our research exhibited CD90 and CD105 while being negative for CD34 and CD45. Previous research [28, 29] found that the CD34 marker was expressed in primitive pluripotent stem cells of both stromal and hemopoietic origin, and it is widely considered as a hemopoietic marker for stem cell populations. in addition, our findings are consistent with those of Suchánek et al., [30] and Kellner et al., [31].

The main culture medium was changed with osteogenic induction media when the DPSC cells achieved 80%-90% confluence for 21 days to evaluate their growth characteristics and osteogenic differentiation ability. They showed excellent differentiation into osteoblasts. In this work, we found considerable morphological changes in induced cultures from fibroblastic to plump and cuboidal-shaped cells. In addition, newly formed osteoblasts formed structured ECM with calcium-rich deposits in vitro, as evidenced by positive staining with "Von Kossa" and Alizarin Red. The findings agreed with those of Graziano et al., [32] and Kermani et al., [33]. On days 14 and 21, PCR was utilized to assess the expression of certain bone-forming gene markers to investigate DPSC differentiation at the mRNA level. Over a 21-day timeframe, the transcription factors RUNX2, osteonectin (ON), and collagen 1 were upregulated in the monolayer of DPSCs under osteogenic conditions. RUNX2 was discovered as an early osteogenesis marker on day 14 and was judged a crucial signal during osteoblast differentiation from DPSCs. RUNX2 also stimulates the expression of ON, an osteogenic differentiation marker. Previous studies assumed that ON is only produced by mature osteoblasts near the conclusion of osteogenic matrix maturation; nevertheless, it may be detected as early as day 14 of osteogenic differentiation.

COL-1 constitutes 90% of the organic matrix. The many osteolytic changes that occur during bone remodeling and collagen breakdown contributed to the identification of COL-1 as a viable bone turnover biomarker. The results we obtained in this experiment were similar to the results of the previous two reviewed studies [36, 37], which showed increased COL-1 production with a dose-dependent increase in matrix mineralization and were thus recognized as specific markers for bone resorption. Osteoblasts deposited additional woven bone (matrix) into the defect around 2 weeks after the initial implantation. Nonetheless, bone mineralization or remodeling began only once the shape of the new bone was adapted to the old tissue [38]. Bone regeneration and remodeling of treated defects were monitored by CT radiograph and histology methods. CT imaging gives three-dimensional data on bone development, whereas histology can only study a two-dimensional portion. [39].In this investigation, macroscopic radiography evaluation revealed the existence of the biomaterial at the defect site, surrounded by a radiolucent edge in the scaffold-only group. At 3 months of healing, there was complete diminution of the radiolucent edge in the bone defects treated with hDPSCs, clearly demonstrating the shift from the reabsorption phase to the repair phase during the healing process. These findings are consistent with the earlier study [40], which found that the radiolucent edge surrounding the biomaterial-containing defects indicates an early phase of bone regeneration in which osteoclasts remove debris from the bone margins, resulting in greater regions of reabsorption. The radiolucent margins fade until they vanish completely, indicating reabsorption impairment and the start of regeneration. Microscopically, the signals of bone regeneration were verified. After three months of a transplant, histological examination revealed that the healing symptoms of the bone deficiency in the area that received a combination of PLGA/HA scaffold and hDPSCs improved. This group was completely regenerated and consisted of well-vascularized bone with a lamellar architecture around the Haversian canals, with a much higher cortical bone level in this area than in the scaffold-only transplant site. Colorado et al., discovered that PLGA/HA scaffolds with chemical and physical characteristics improved hDPSC adhesion, growth, and differentiating towards the osteogenic lineage and encouraged critical-size osseous defect repair in vivo when used as an alternative biomaterial with hDPSc-PLGA/HA scaffold. [41]. Furthermore, in the groups that only got the PLGA/HA scaffold, a more immature bone was created. The empty control group, on the other hand, showed little new bone formation with several unhealed cavities [newly formed bone marrow]. These findings are consistent with earlier research. According to Zhang et al., Because of its conductive action, HA has been widely used in bone scaffolds and is frequently used in clinical practise, either directly or in conjunction with other materials. Modified HA particles may aid to stabilize the mechanical properties of PLGA scaffolds by extending the calcium surface for osteoblast ossification. [42].However, the findings of our investigation not in line with what the previous review [43] reported when HA is applied alone in a critical-size rat defect without the inclusion of stem cells, it has a higher proportion of marrow gaps and results in less bone growth than deproteinized bovine bone [DGB]. When compared to the other groups studied, immunohistochemical labeling revealed enhanced mature lamellar bone content in PLGA/HA/hDPSC-treated defects, as well as better histological feature recovery and high immunoexpression for collagen type I. This demonstrates that the higher fiber content led to good tissue quality with optimal support and structure, facilitating bone mineralization.

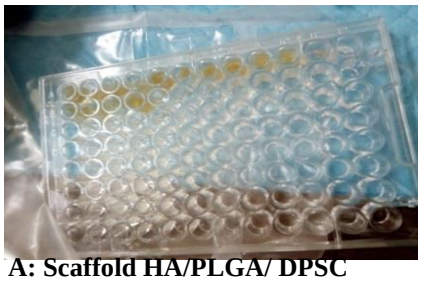

A: Scaffold HA/PLGA/ DPSC before its placement

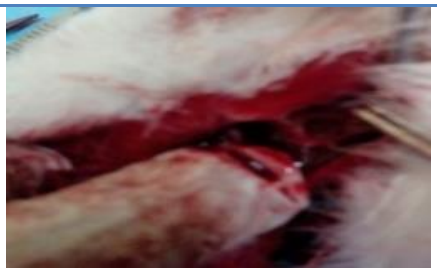

B: The mandibular periosteum Was elevated.

C: A circle bone segment (3-cm defect) was removed:

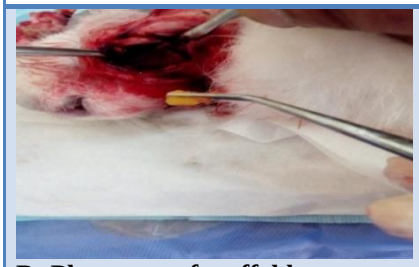

D: Placement of scaffold HA/PLGA/HDPSC in the surgical side

: Placement of scaffold HA/PLGA/ in the in the surgical site:

G: Suture by layers with silk 4-0

Figure 1: Methods of surgical procedure

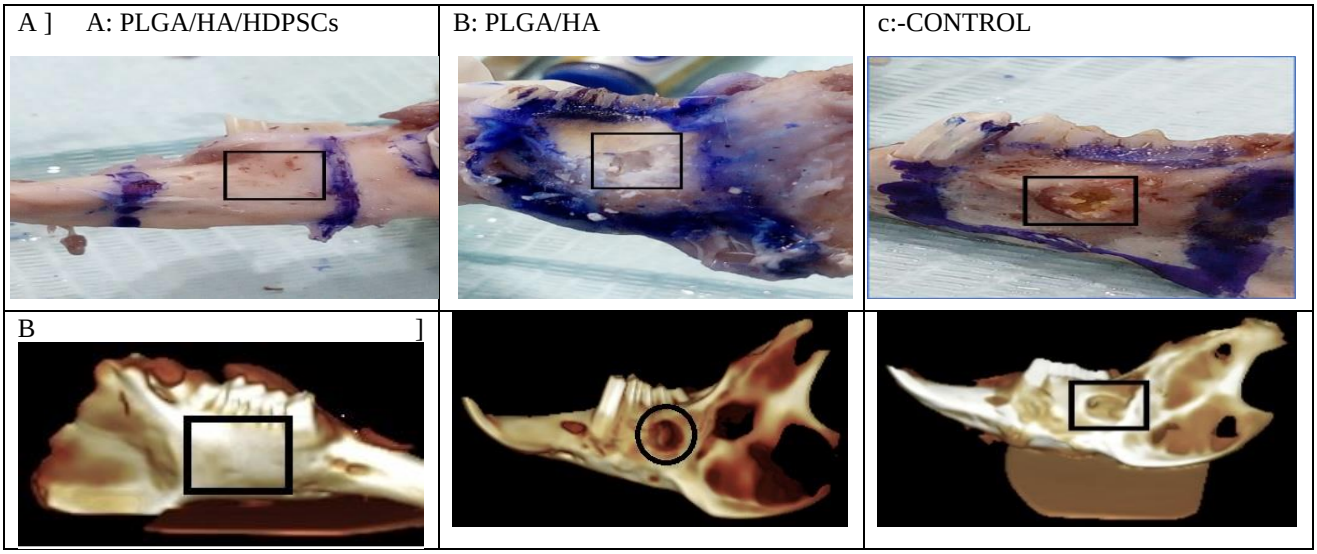

Figure 2: A- The group 1 presented filling of the defect area with tissue of hard consistency, compatible with satisfactory macroscopic bone healing was observed after 3 months. (B) In the group II the defect was partially filled with callus bone, while a large proportion of the residual scaffold was observed in the defect site at 3 months after implantation. (C) The control defects presented a soft consistency due to the failure in the ossification and the presence of fibrous tissues at 3 months after implantation. B- The group 1 presented a more intense radiopaque signal at the lesion site, indicating greater density of newly formed bone and was difficult to differentiate from the original surrounding bone. (B) In the group II the defect presented a more radiolucent defect filling, indicating a less competent matrix formation for the newly formed bone. (C) The control defects presented a radiolucent circle inside defect, thus, confirming .The lesion model as a critical bone defect.

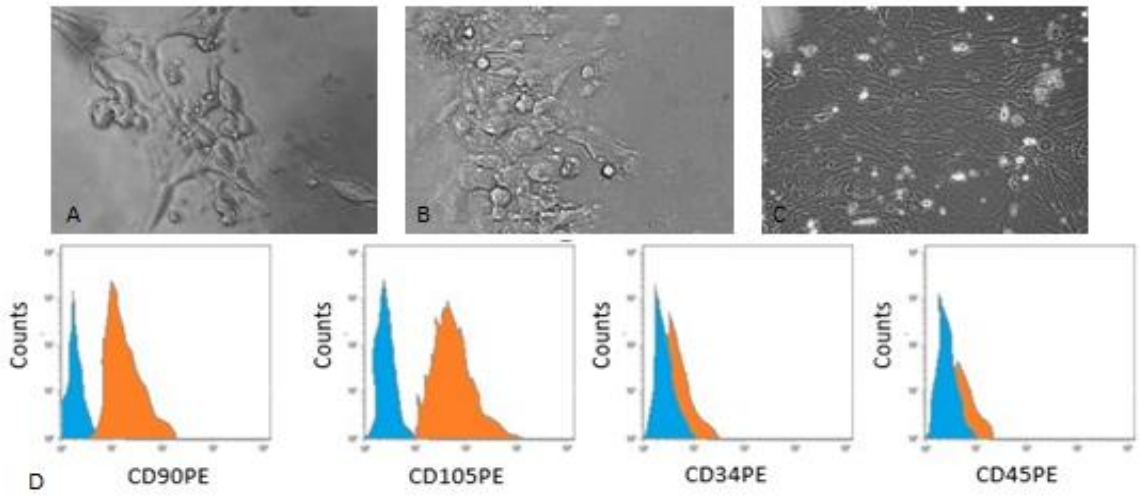

A: DPSCs were cultured at day 7, B:DPSCs were cultured at day 14, C:DPSCs were cultured at day 21 and E: DPSCs were characterized by FACS; they were positive for CD90 and CD105 AND they were negative for CD34 and CD45.

Figure 3: Differentiation potential of DPSCs:- A) Controlled, B&C)Von Kossa staining at day 14 and 21 respectively confirming mineral deposition by newly formed osteoblasts, D) Alizarin red staining at day 21.

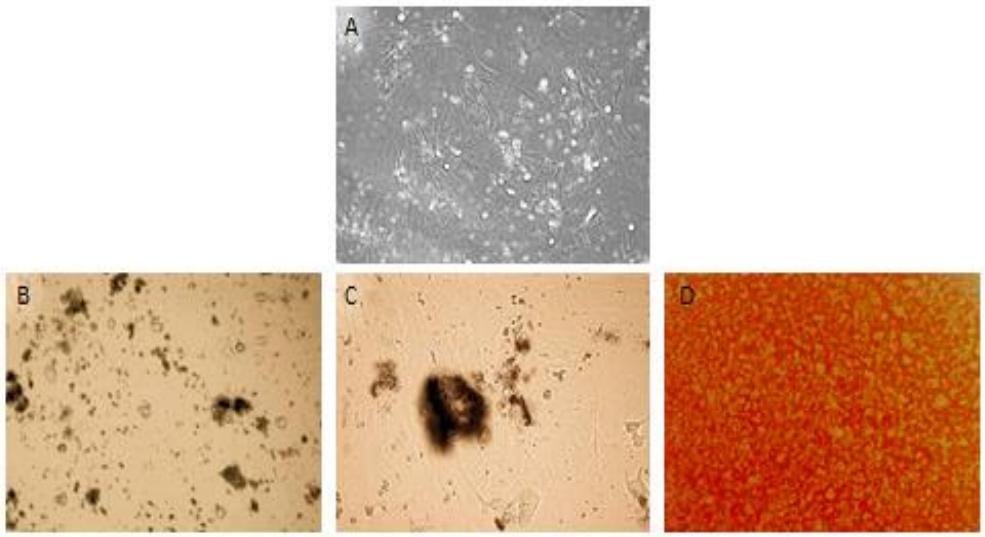

Differentiation potential of DPSCs. A) controlled, B, C) Von kossa staining at day 14 and 21 respectivly, confirming mineral deposition by newly formed osteoblasts D) alizarin red staining at day 21.

Figure 4: Dental pulp stem cell culture at 4-7 days, B): at two weeks, C): at three weeks, D: FACS; they were positive for CD90 and CD105 and they were negative for CD34 and CD45.

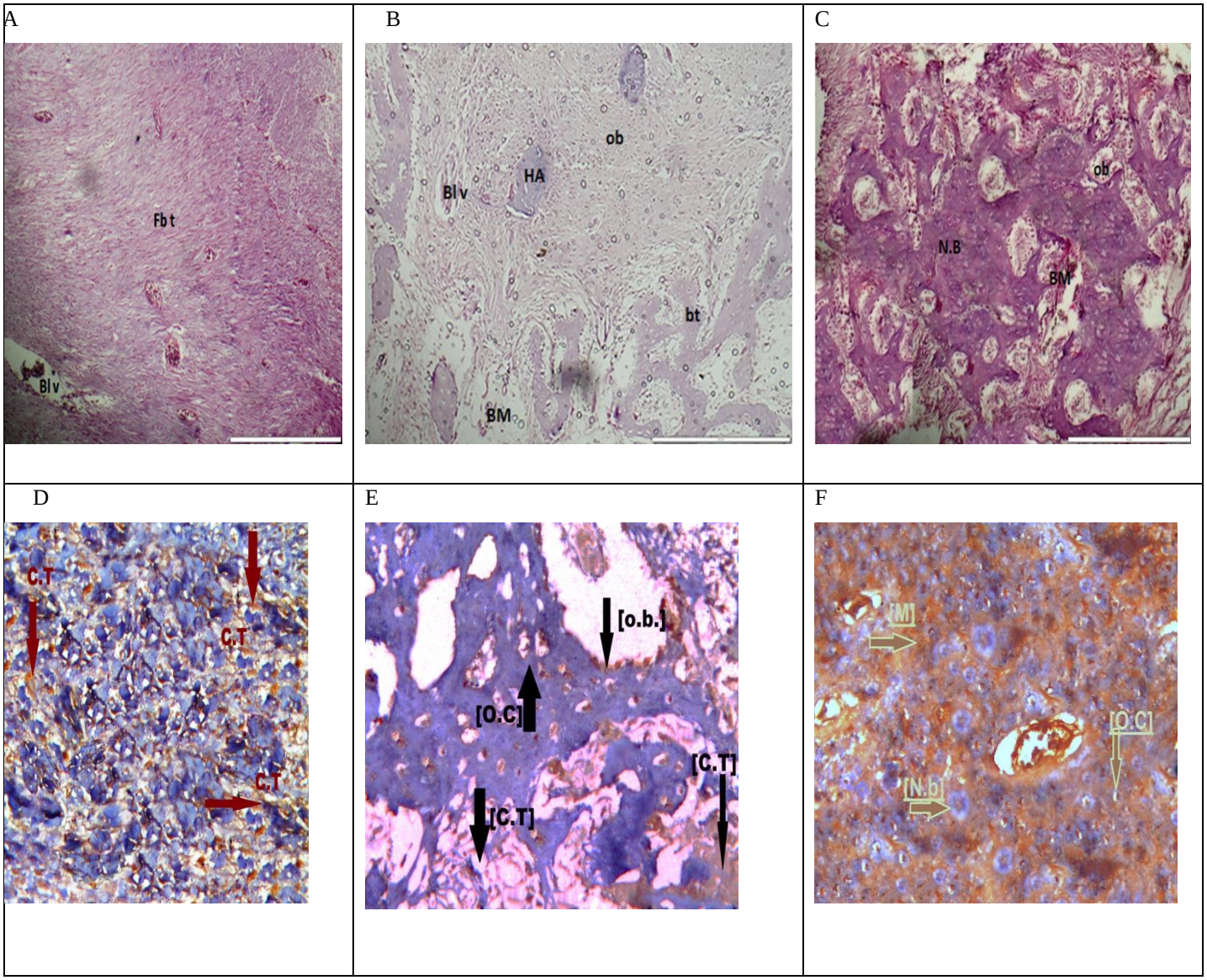

Figure 5: Photomicrographs of decalcified section in the critical sized of mandibular defect in the four experimental groups after 3 months of implantation. (A) Control group [empty bone defect showing fibrous tissue scar[F.t] (B) PLGA/HA scaffold only group showing newly formed bone tissue[o.b] with wide bone marrow spaces[B.M] and new vascularization [v] and HA particles [HA], (C] PLGA/HA/HDPSCs group showing newly formed compact bone composed of osteon , Haversian canal [H.S] lamellar bone [b.l], osteocyte [O.c] and osteoblast lining the surface of newly formed bone [o.B]. Coloration: hematoxylin and eosin (HE), Mag 100x]

Photomicrographs of decalcified section in the critical sized of mandibular defect in the threeexperimental groups after 3 months of implantation. (D) Control group showed negative immunoreactivity and fibrous connective tissue showed positive immunoreactivity .[C.T] (E) PLGA/HA scaffold only group showed the newly formed bone in the central areas of the defect, the osteoblasts along the surface [o.B], and osteocytes[o.c] displayed moderately positive immunoreactivity .Moreover, the connective tissue fibroblasts showed variable staining, [C.T]. (F) PLGA/HA/HDPSCs group showed intense immunoreactivity in areas of new bone formation within the defect region in the osteoid seam. [Immunohistochemistry of Collagen type 1 Mag 200 x].

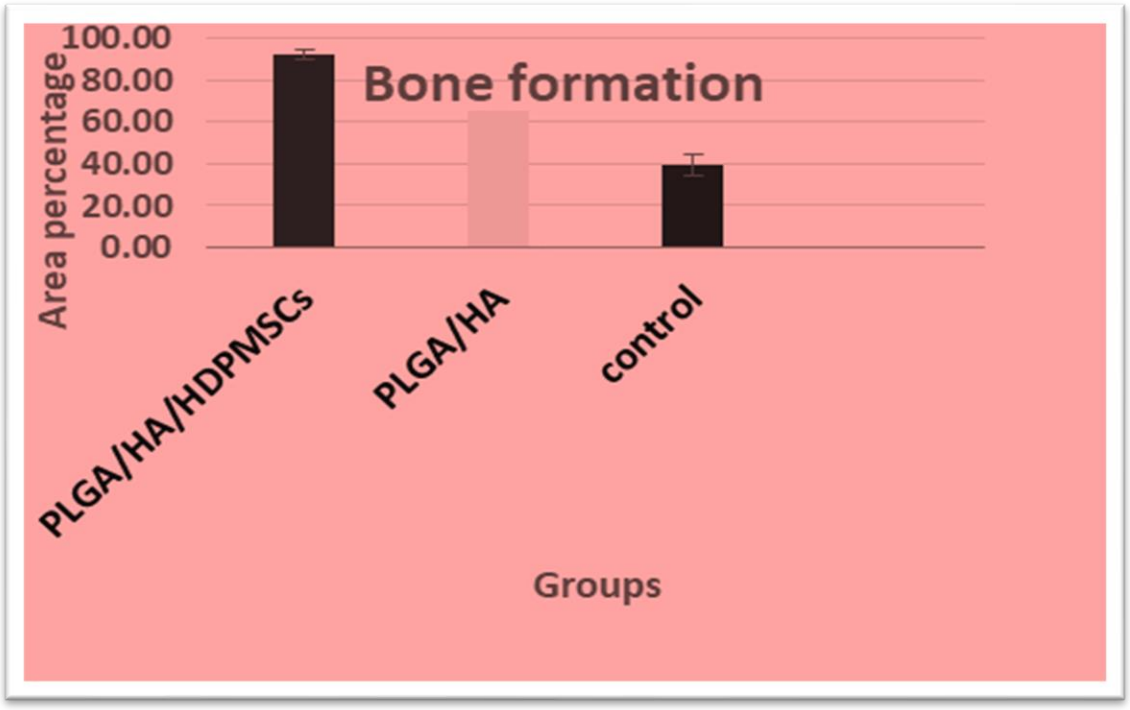

Figure 6: Bar chart representing bone formation for the three experimental groups

Table 1: List of used primers and their sequences

Gene symbol	Primer sequence from 5′- 3′
RUNX2	F: ATGCATTTAAGATATGGTTGCC R: TGGAGTTGGGAAACACTTGA
ON	F: CGAGCTGGATGAGAACAACA R: AAGTGGCAGGAAGAGTCGAA
COL I	F: GATGCGTTCCAGTTCGAGTA R: GGTCTTCCGGTGGTCTTGTA
GAPDH	F: ATCGTGCGGGACATCAA R: AGGAAGGAGGGCTGGAA

The following PCR conditions were used; denaturation for 5 minutes at 95°C; followed by annealing for 30 seconds at 55°C and extension at 72°C. PCR products were visualized by agarose gel electrophoresis

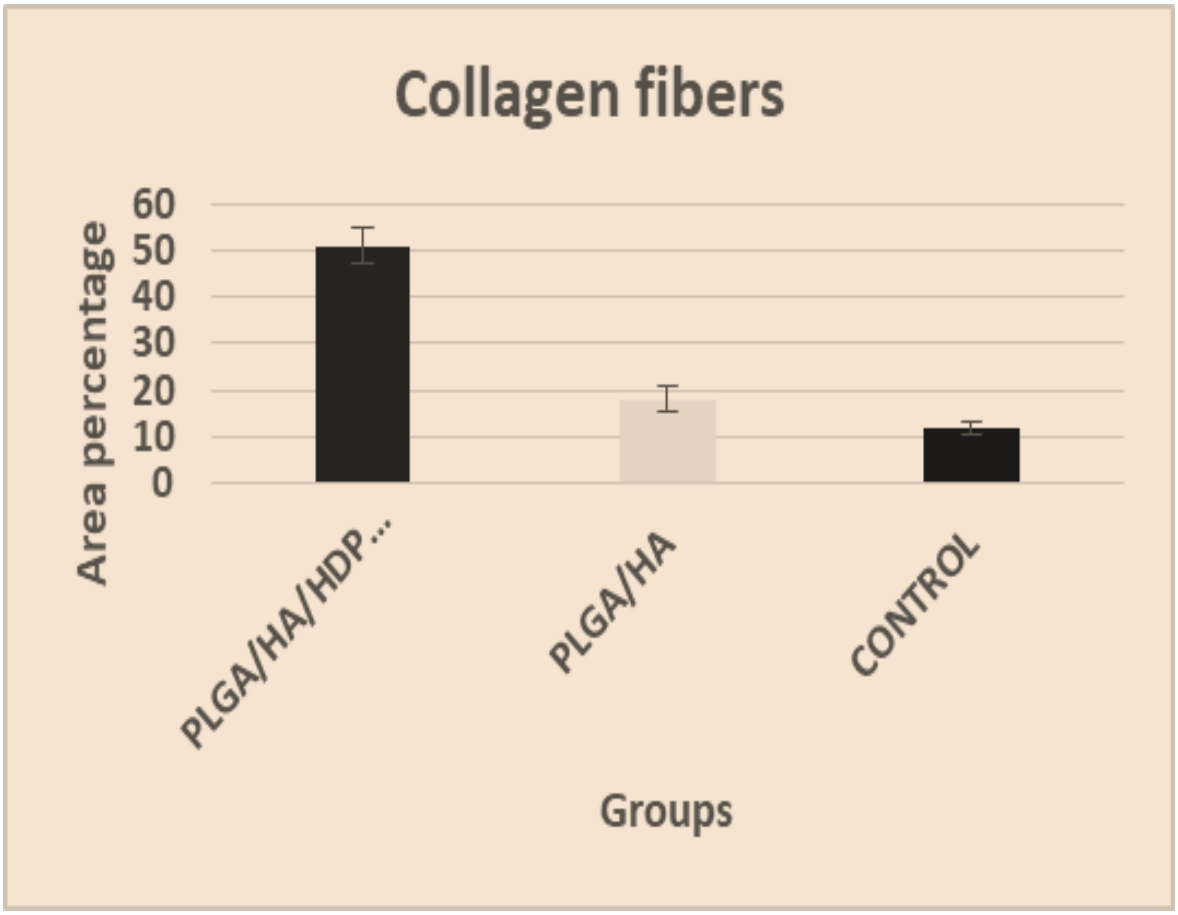

Figure 7: Bar chart representing collagen fibers in the three experimental groups

Our results may be contrasted to those of Pinheiro et al., and Attia et al., who used HA/-TCP and micro-HA scaffolds, respectively. They detected an increase in collagen fiber and HA deposition, suggesting that the biomaterial caused a response in the healing process. [44, 45].

5. Conclusions

Stem cell therapy is emerging as a revolutionary treatment modality to treat diseases and injuries, with wide-ranging medical benefits. According to the present study, HDPSCs have the ability to develop into more types of body tissue than other types of stem cells. This difference opens the door to more therapeutic applications. Also, the existing research has clearly shown that the third molars of permanent teeth are a better source for stem cells .

Declarations Section

A- Author Contribution

The conception and design of the study was done by Khalaf, Afaf, data analysis was done by Ali, Shamaa drafting, and revising manuscript were done by Ali, Sabry, Dina, Abd El Fattah, Saher S, Mohammed.

B- Funding

No specific grant was given to this study by funding organizations in public, private, or not-for-profit sectors.

C. Conflict of interest

The authors claim to have no conflicts of interest.

Acknowledgments

I would like to thank all staff members of Biology at Faculty of Oral and Dental Medicine, Minia University for their cooperation.

References

[1] U. Kneser, D.J. Schaefer, E. Polykandriotis, R.E. Horch. (2006). Tissue engineering of bone: the reconstructive surgeon's point of view. Journal of cellular and molecular medicine. 10(1): 7-19.

[2] A. Oryan, S. Alidadi, A. Moshiri, N. Maffulli. (2014). Bone regenerative medicine: classic options, novel strategies, and future directions. Journal of orthopaedic surgery and research. 9(1): 1-27.

[3] U. Kneser, D. Schaefer, B. Munder, C. Klemt, C. Andree, G. Stark. (2002). Tissue engineering of bone. Minimally Invasive Therapy & Allied Technologies. 11(3): 107-116.

[4] T. Ghassemi, A. Shahroodi, M.H. Ebrahimzadeh, A. Mousavian, J. Movaffagh, A. Moradi. (2018). Current concepts in scaffolding for bone tissue

engineering. Archives of bone and joint surgery. 6(2): 90.
[5] A.J. Salgado, O.P. Coutinho, R.L. Reis. (2004). Bone tissue engineering: state of the art and future trends. Macromolecular bioscience. 4(8): 743-765.
[6] J. Mitra, G. Tripathi, A. Sharma, B. Basu. (2013). Scaffolds for bone tissue engineering: role of surface patterning on osteoblast response. RSC advances. 3(28): 11073-11094.
[7] G.L. Koons, M. Diba, A.G. Mikos. (2020). Materials design for bone-tissue engineering. Nature Reviews Materials. 5(8): 584-603.
[8] G. Laino, A. Graziano, R. d'Aquino, G. Pirozzi, V. Lanza, S. Valiante, A. De Rosa, F. Naro, E. Vivarelli, G. Papaccio. (2006). An approachable human adult stem cell source for hard-tissue engineering. Journal of cellular physiology. 206(3): 693-701.
[9] C.A. Heath. (2000). Cells for tissue engineering. Trends in biotechnology. 18(1): p. 17-19.
[10] J.R. Mauney, V. Volloch, D.L. Kaplan. (2005). Role of adult mesenchymal stem cells in bone tissue engineering applications: current status and future prospects. Tissue engineering. 11(5-6): 787-802.
[11] J.L. Lansdowne, D. Devine, U. Eberli, P. Emans, T.J. Welting, J.C. Odekerken, D. Schiuma, M. Thalhauser, L. Bouré, S. Zeiter. (2014). Characterization of an ovine bilateral critical sized bone defect iliac wing model to examine treatment modalities based on bone tissue engineering. BioMed research international.
[12] N. Zwetyenga, S. Catros, A. Emparanza, C. Deminiere, F. Siberchicot, J.-C. Fricain. (2009). Mandibular reconstruction using induced membranes with autologous cancellous bone graft and HA-βTCP: animal model study and preliminary results in patients. International journal of oral and maxillofacial surgery. 38(12): 1289-1297.
[13] K. Akiyama, C. Chen, S. Gronthos, S. Shi. (2012). Lineage differentiation of mesenchymal stem cells from dental pulp, apical papilla, and periodontal ligament. Odontogenesis: Methods and Protocols. 111-121.
[14] J.-H. Li, D.-Y. Liu, F.-M. Zhang, F. Wang, W.-K. Zhang, Z.-T. Zhang. (2011). Human dental pulp stem cell is a promising autologous seed cell for bone tissue engineering. In Chinese Medical Journals Publishing House Co., Ltd. 42 Dongsi Xidaji. Vol. 124, pp 4022-4028.
[15] A. Francia, G. Grazioli, L. Echarte, Á. Maglia, C. Touriño, I. Alvarez. (2021). Establishing and implementing a simplified protocol for the expansion and culture of human dental pulp stem cells (hDPSCs). Odontoestomatología. 23(38).
[16] A. Zimina, F. Senatov, R. Choudhary, E. Kolesnikov, N. Anisimova, M. Kiselevskiy, P. Orlova, N. Strukova, M. Generalova, V. Manskikh. (2020). Biocompatibility and physico-chemical properties of highly porous PLA/HA scaffolds for bone reconstruction. Polymers. 12(12): 2938.
[17] S. Awais, S.S. Balouch, N. Riaz, M.S. Choudhery. (2020). Human dental pulp stem cells exhibit osteogenic differentiation potential. Open life sciences. 15(1): 229-236.
[18] P. Kasten, J. Vogel, F. Geiger, P. Niemeyer, R. Luginbühl, K. Szalay. (2008). The effect of platelet-rich plasma on healing in critical-size long-bone defects. Biomaterials. 29(29): 3983-3992.
[19] A. Alkaisi, S.S. Mutum, Z.A.R. Ahmad, S.A. Masudi, N.H. Abd Razak. (2013). Transplantation of human dental pulp stem cells: enhance bone consolidation in mandibular distraction osteogenesis. Journal of Oral and Maxillofacial Surgery. 71(10): 1758. e1-1758. e13.
[20] R. Kassir, A. Kolluru, M. Kassir. (2011). Intense pulsed light for the treatment of rosacea and telangiectasias. Journal of Cosmetic and Laser Therapy. 13(5): 216-222.
[21] C. Llena, M. Collado-González, C.J. Tomás-Catalá, D. García-Bernal, R.E. Oñate-Sánchez, F.J. Rodríguez-Lozano, L. Forner. (2018). Human dental pulp stem cells exhibit different biological behaviours in response to commercial bleaching products. Materials. 11(7): 1098.
[22] R. Dimitriou, E. Jones, D. McGonagle, P.V. Giannoudis. (2011). Bone regeneration: current concepts and future directions. BMC medicine. 9(1): 1-10.
[23] H.E. Jazayeri, M. Tahriri, M. Razavi, K. Khoshroo, F. Fahimipour, E. Dashtimoghadam, L. Almeida, L. Tayebi. (2017). A current overview of materials and strategies for potential use in maxillofacial tissue regeneration. Materials Science and Engineering: C. 70: 913-929.
[24] M. Dang, L. Saunders, X. Niu, Y. Fan, P.X. Ma. (2018). Biomimetic delivery of signals for bone tissue engineering. Bone research. 6(1): 25.
[25] D. Kim, A.E. Lee, Q. Xu, Q. Zhang, A.D. Le. (2021). Gingiva-derived mesenchymal stem cells: potential application in tissue engineering and regenerative medicine-a comprehensive review. Frontiers in immunology. 12: 667221.
[26] S.H. Park, D.S. Park, J.W. Shin, Y.G. Kang, H.K. Kim, T.R. Yoon, J.-W. Shin. (2012). Scaffolds for bone tissue engineering fabricated from two different materials by the rapid prototyping technique: PCL versus PLGA. Journal of Materials Science: Materials in Medicine. 23: 2671-2678.
[27] Z. Pan, J. Ding. (2012). Poly (lactide-co-glycolide) porous scaffolds for tissue engineering and regenerative medicine. Interface focus. 2(3): 366-377.
[28] R. Farahzadi, E. Fathi, S.A. Mesbah-Namin, N. Zarghami. (2018). Anti-aging protective effect of L-carnitine as clinical agent in regenerative medicine through increasing telomerase activity and change in the hTERT promoter CpG island methylation status of adipose tissue-derived mesenchymal stem cells. Tissue and Cell. 54: 105-113.
[29] E. Fathi, R. Farahzadi, B. Valipour, Z. Sanaat. (2019). Cytokines secreted from bone marrow derived mesenchymal stem cells promote apoptosis

and change cell cycle distribution of K562 cell line as clinical agent in cell transplantation. PLoS One. 14(4): e0215678.

[30] J. Suchánek, T. Soukup, R. Ivancakova, J. Karbanová, V. Hubková, R. Pytlík, L. Kucerova. (2007). Human dental pulp stem cells-isolation and long term cultivation. ACTA MEDICA-HRADEC KRALOVE-. 50(3): 195.

[31] M. Kellner, M.M. Steindorff, J.F. Strempel, A. Winkel, M.P. Kühnel, M. Stiesch. (2014). Differences of isolated dental stem cells dependent on donor age and consequences for autologous tooth replacement. Archives of oral biology. 59(6): 559-567.

[32] R. d'Aquino, G. Papaccio, G. Laino, A. Graziano. (2008). Dental pulp stem cells: a promising tool for bone regeneration. Stem cell reviews. 4: 21-26.

[33] S. Kermani, R.M.A. Wahab, I.Z.Z. Abidin, Z.Z. Ariffin, S. Senafi, S.H.Z. Ariffin. (2014). Differentiation capacity of mouse dental pulp stem cells into osteoblasts and osteoclasts. Cell Journal (Yakhteh). 16(1): 31.

[34] P. Hilkens, P. Gervois, Y. Fanton, J. Vanormelingen, W. Martens, T. Struys, C. Politis, I. Lambrichts, A. Bronckaers. (2013). Effect of isolation methodology on stem cell properties and multilineage differentiation potential of human dental pulp stem cells. Cell and tissue research. 353(1): 65-78.

[35] E. Bressan, L. Ferroni, C. Gardin, P. Pinton, E. Stellini, D. Botticelli, S. Sivolella, B. Zavan. (2012). Donor age-related biological properties of human dental pulp stem cells change in nanostructured scaffolds. PLoS One. 7(11): e49146.

[36] M. Osugi, W. Katagiri, R. Yoshimi, T. Inukai, H. Hibi, M. Ueda. (2012). Conditioned media from mesenchymal stem cells enhanced bone regeneration in rat calvarial bone defects. Tissue engineering part A. 18(13-14): 1479-1489.

[37] A.P. Barhanpurkar, N. Gupta, R.K. Srivastava, G.B. Tomar, S.P. Naik, S.R. Joshi, S.T. Pote, G.C. Mishra, M.R. Wani. (2012). IL-3 promotes osteoblast differentiation and bone formation in human mesenchymal stem cells. Biochemical and biophysical research communications. 418(4): 669-675.

[38] J.C. Esteves, E. Marcantonio Jr, A.P. de Souza Faloni, F.R.G. Rocha, R.A. Marcantonio, K. Wilk, G. Intini. (2013). Dynamics of bone healing after osteotomy with piezosurgery or conventional drilling–histomorphometrical, immunohistochemical, and molecular analysis. Journal of translational medicine. 11(1): 1-13.

[39] S. Annibali, R. Quaranta, A. Scarano, A. Pilloni, A. Cicconetti, M.P. Cristalli, D. Bellavia, L. Ottolenghi. (2016). Histomorphometric evaluation of bone regeneration induced by biodegradable scaffolds as carriers for dental pulp stem cells in a rat model of calvarial" critical size" defect. Journal of stem cell research and therapy. 6(1): 1-8.

[40] K.M. Nuss, B. von Rechenberg. (2008). Biocompatibility issues with modern implants in bone-a review for clinical orthopedics. The open orthopaedics journal. 2: 66.

[41] C. Colorado, L.M. Escobar, G.I. Lafaurie, C. Durán, S.J. Perdomo-Lara. (2022). Human recombinant cementum protein 1, dental pulp stem cells, and PLGA/hydroxyapatite scaffold as substitute biomaterial in critical size osseous defect repair in vivo. Archives of oral biology. 137: 105392.

[42] D. Zhang, X. Wu, J. Chen, K. Lin. (2018). The development of collagen based composite scaffolds for bone regeneration. Bioactive materials. 3(1): 129-138.

[43] S. Annibali, D. Bellavia, L. Ottolenghi, A. Cicconetti, M.P. Cristalli, R. Quaranta, A. Pilloni. (2014). Micro-CT and PET analysis of bone regeneration induced by biodegradable scaffolds as carriers for dental pulp stem cells in a rat model of calvarial "critical size" defect: Preliminary data. Journal of Biomedical Materials Research Part B: Applied Biomaterials. 102(4): 815-825.

[44] A.L.B. Pinheiro, M.E. Martinez Gerbi, F. de Assis Limeira, E.A. Carneiro Ponzi, A.M. Marques, C.M. Carvalho, R. de Carneiro Santos, P.C. Oliveira, M. Nóia, L.M.P. Ramalho. (2009). Bone repair following bone grafting hydroxyapatite guided bone regeneration and infra-red laser photobiomodulation: a histological study in a rodent model. Lasers in medical science. 24: 234-240.

[45] M.S. Attia, H.M. Mohammed, M.G. Attia, M.A.A.E. Hamid, E.A. Shoeriabah. (2019). Histological and histomorphometric evaluation of hydroxyapatite-based biomaterials in surgically created defects around implants in dogs. Journal of Periodontology. 90(3): 281-287.